View metadata, citation and similar papers at core.ac.uk

brought to you by CORE

provided by Purdue E-Pubs

Purdue University
Purdue e-Pubs

Birck and NCN Publications | Birck Nanotechnology Center

4-1-2011

Electronic structure, vibrational spectrum, and thermal properties of yttrium nitride: A first-principles study

Bivas Saha
Birck Nanotechnology Center, Purdue University, bsaha@purdue.edu

Timothy D. Sands
Birck Nanotechnology Center, Purdue University, tsands@purdue.edu

Umesh V. Waghmare
Jawaharlal Nehru Center for Advanced Scientific Research

Follow this and additional works at: http://docs.lib.purdue.edu/nanopub


Part of the Nanoscience and Nanotechnology Commons

Saha, Bivas; Sands, Timothy D.; and Waghmare, Umesh V., "Electronic structure, vibrational spectrum, and thermal properties of yttrium nitride: A first-principles study" (2011). *Birck and NCN Publications.* Paper 1030.
http://dx.doi.org/10.1063/1.3561499

This document has been made available through Purdue e-Pubs, a service of the Purdue University Libraries. Please contact epubs@purdue.edu for additional information.

AIP | Journal of Applied Physics

Electronic structure, vibrational spectrum, and thermal properties of yttrium nitride: A first-principles study

Bivas Saha, Timothy D. Sands, and Umesh V. Waghmare

Citation: J. Appl. Phys. **109**, 073720 (2011); doi: 10.1063/1.3561499
View online: http://dx.doi.org/10.1063/1.3561499
View Table of Contents: http://jap.aip.org/resource/1/JAPIAU/v109/i7
Published by the AIP Publishing LLC.

Additional information on J. Appl. Phys.

Journal Homepage: http://jap.aip.org/
Journal Information: http://jap.aip.org/about/about_the_journal
Top downloads: http://jap.aip.org/features/most_downloaded
Information for Authors: http://jap.aip.org/authors

ADVERTISEMENT

Downloaded 16 Aug 2013 to 128.46.221.64. This article is copyrighted as indicated in the abstract. Reuse of AIP content is subject to the terms at: http://jap.aip.org/about/rights_and_permissions

Electronic structure, vibrational spectrum, and thermal properties of yttrium nitride: A first-principles study

Bivas Saha,[1,2,a)] Timothy D. Sands,[1,2,3] and Umesh V. Waghmare[4]
[1]*School of Materials Engineering, Purdue University, West Lafayette, Indiana 47907, USA*
[2]*Birck Nanotechnology Center, Purdue University, West Lafayette, Indiana 47907, USA*
[3]*School of Electrical and Computer Engineering, Purdue University, West Lafayette, Indiana 47907, USA*
[4]*Theoretical Sciences Unit, Jawaharlal Nehru Centre for Advanced Scientific Research, Jakkur, Bangalore 560064, India*

(Received 30 November 2010; accepted 8 February 2011; published online 8 April 2011)

Yttrium nitride (YN) is a promising semiconductor for use in metal/semiconductor superlattices for thermoelectric applications. We determine its electronic structure, vibrational spectrum, and thermal properties using first-principles density functional theory (DFT) based simulations with a generalized gradient approximation (GGA) of the exchange correlation energy. We employ GGA+U and GW approximations in our calculations to (a) improve the accuracy of the calculation of bandgaps and (b) determine specific features of its electronic structure relevant to transport properties, such as transverse (m_t*) and longitudinal (m_l*) conduction band effective mass. To evaluate consequences of forming alloys of YN with other materials to its electronic properties, we have determined the volume deformation potentials. Our results for phonons show a large longitudinal optical (LO) and transverse optical (TO) splitting at the Γ point in the vibrational spectrum with a gap of 325 cm^{-1} arising from long- range dipole-dipole interactions. We estimate temperature dependent lattice specific heat and lattice thermal conductivity based on Boltzmann transport theory to assess YN's potential for thermoelectric applications. © *2011 American Institute of Physics*. [doi:10.1063/1.3561499]

I. INTRODUCTION

Early transition nitride materials are very hard, chemically stable and possess high corrosion resistance.[1–4] They are also interesting from a fundamental point of view due to their unusual and diverse properties. They have a wide range of applications, from cutting tools and protective coatings to hard coating for magnetic storage devices. Recently, much research effort is being invested in understanding their potential for energy and environment related applications.[5,6]

Yttrium nitride (YN) crystallizes in the rock salt structure and is a promising material for thermoelectric and thermionic applications. It is of current interest and is being studied experimentally to tune electrical and thermal properties through the formation of alloys with other nitride materials. Although there are first-principles based studies[7–9] on the structure and the electronic properties of YN, the estimate of its bandgap is multivalued and unclear. Moreover, the transport related properties like transverse and longitudinal conduction band effective mass have not been estimated yet. It is also necessary to enumerate its different volume deformation potentials. We note a recent work of Isaev *et al.*,[10] where they determined vibrational spectra of YN. Here we benchmark our work through comparison with theirs and take it forward to estimate thermal properties such as lattice specific heat and lattice thermal conductivity, and compare it with that of ScN and rationalize its suitability for mixing with ScN in technological applications.

Density functional theory (DFT) calculations based on local-density approximation (LDA) and generalized gradient approximation (GGA) are well known for underestimation of bandgaps of semiconductors or insulators. In particular for transition nitride materials, their performance would be considered poor. Both in the case of YN and ScN, standard GGA based calculations show semimetallic or semiconducting nature with the Γ-X bandgap of 0.2−0.3 eV.[7,11] Several techniques have been developed over the years to correct this bandgap problem with examples like screened-exchange LDA.[8] (LDA, GGA) + U,[12] and GW[13,14] approximation and others. While the (LDA, GGA) + U technique takes into account the on-site Hubbard interaction correction, the GW approximation works by taking into account the self-energy correction and is established to be a reliable technique to correctly estimate bandgaps of semiconductors. Rather than solving the Kohn-Sham equations, one solves the Dyson's equation in the GW approach taking into account the self energy corrections, although self-consistency in GW is still a matter of debate and tends to produce higher estimates of bandgap.

In this work, we present a combination of the GGA + U and the GW approaches to estimate the bandgap, volume deformation potential, and transverse and longitudinal conduction band effective masses of YN. The GGA-based calculation is used to estimate vibrational spectra, lattice specific heat, and lattice thermal conductivity and its variation with temperature to understand YN's suitability and potential for thermoelectric applications.

a)Electronic mail: bsaha@purdue.edu.

 © 2011 American Institute of Physics

Downloaded 16 Aug 2013 to 128.46.221.64. This article is copyrighted as indicated in the abstract. Reuse of AIP content is subject to the terms at: http://jap.aip.org/about/rights_and_permissions

II. METHODS OF CALCULATION

We use the plane wave self consistent field (PWSCF) implementation of density functional theory (DFT) with a generalized gradient approximation (GGA)[15,16] to exchange correlation energy and ultrasoft pseudopotential[17] to represent the interaction between ionic cores and valence electrons. A plane wave basis set (PWs) with cut-off energy of 30 Ry was used to represent the electronic wave functions, and PWs with an energy cutoff of 180 Ry were included for the representation of charge density. Integration over the Brillouin zone was carried out using the Monkhorst-Pack[18] scheme with a $10 \times 10 \times 10$ mesh of k-points, and occupation numbers were smeared according to the Methfessel-Paxton[19] scheme with a broadening of 0.003 Ry. Hubbard U corrections are included along with GGA in determination of the electronic structure of YN, particularly the bandgap.

Lattice-dynamical calculations (phonon spectrum, density of states) were performed within the framework of the self-consistent density functional perturbation theory.[20] Plane wave basis sets with cutoff energies of 40 and 750 Ry were used to describe wave functions and charge density, respectively. Such high energy cutoffs are necessary to keep the errors in vibrational frequencies of nitrides low.[21] Integration over the Brillouin zone is performed using an $18 \times 18 \times 18$ mesh of k-points. To understand detailed features of phonon spectra, force constant matrices (K) are obtained on a $4 \times 4 \times 4$ q-point mesh. The dynamical matrices at arbitrary wave vectors are determined using Fourier transform based interpolations of force constant matrices to obtain phonon dispersion.

The specific heat Cp and thermal conductivity κ are given by

$$C_p = \frac{1}{N_q}\sum_{\lambda q}\left[k_B\left(\frac{\hbar\omega_{\lambda q}}{k_B T}\right)^2 \frac{e^{\hbar\omega_{\lambda q}/k_B T}}{\left(e^{\hbar\omega_{\lambda q}/k_B T}-1\right)^2}\right] \quad (1)$$

$$\kappa_{\alpha\beta} = \hbar\sum_{\lambda}\int \frac{d^3q}{(2\pi)^3} v_{\alpha\lambda}(q) v_{\beta\lambda}(q)\omega_\lambda(q)\tau_\lambda(q)\left\{\frac{dn_B[\omega\lambda(q)]}{dT}\right\} \quad (2)$$

where $v_{\beta\lambda}$ (q) is the velocity of the phonon, τ_λ (q) is the relaxation time, and n_B $[\omega_\lambda(q)]$ is the Bose-Einstein distribution function. The relaxation time τ_λ (q) is assumed to be constant and taken outside the integral. Eigen-frequencies were obtained in a dense mesh of k-points over the entire Brillouin zone that were subsequently used in determining $v_{\alpha\lambda}$ (q) using first order finite difference formula.

GW calculations have been carried out using the VASP package[22] of the density functional theory with PAW-GGA potentials to represent the interaction between ionic cores and valence electrons. Integration over the Brillouin zone was performed using an $8 \times 8 \times 8$ mesh of k-points and an energy cutoff of 400 eV was used on the plane wave basis. The GW self- energy operator, $\Sigma = iGW$, where G is the Greens function and W is the screened Coulomb interaction, is constructed from the GGA results.

TABLE I. Calculated lattice constant a (Å) and bulk modulus (B) of YN. Results of our calculations are presented in first two rows, followed by literature values.

Methodology	A(Å)	B(GPa)
GGA	4.90	160
PAW-GGA	4.93	163
FLAPW-GGA (Ref. 6)	4.85	163
Expt. (Ref. 21)	4.87	-

III. RESULTS

A. Crystal structure

Like other transition nitrides, YN crystallizes in the rock salt structure under ambient conditions. Our estimates of lattice constant and bulk modulus (see Table I) are within typical DFT errors of experimental values. Our estimate of lattice constant with the PWSCF based GGA calculation yields a value closer to experiment[23] than VASP-based PAW-GGA calculations. The bulk modulus is in reasonable agreement with both the methods employed and also compares well with an all-electron theoretical investigation[8] giving us confidence in our calculation approach.

B. Electronic structure

To determine electronic properties of YN, we have estimated direct and indirect bandgaps with the GGA and GGA + U calculations and projector augmented wave basis set for GW approximation calculations. Though there are first-principles based reports on the bandgap of YN,[7,8] there has been no consensus on its electronic structure. Our density functional theory calculations within the generalized gradient approximation show that YN is an indirect bandgap semiconductor with the indirect Γ-X bandgap of 0.21 eV, and direct gaps at the Γ and X point being 0.60 and 3.14 eV, respectively. Similar results were also indicated by Mancera *et al.*,[7] using all electron based FP-LAPW calculations. Their work suggests an indirect Γ-X bandgap of 0.31 eV, while direct gaps at the Γ and X points being 0.62 and 3.10 eV, respectively. The screened exchange LDA calculation of

TABLE II. Estimated direct and indirect band gaps at different regions of the dispersion spectrum using GGA coupled with a Hubbard U parameter and increasing U values. m_l* and m_t* represents longitudinal and transverse conduction band effective mass at the X point of the dispersion spectrum.

U(eV)	$E_{\Gamma-X}$(eV)	E_X(eV)	E_Γ(eV)	m_l* (m_0)	m_t* (m_0)
0.0	0.21	0.60	3.14	1.31	0.141
0.5	0.37	0.77	3.20	1.37	0.162
1.0	0.45	0.85	3.23	1.41	0.174
1.5	0.54	0.94	3.27	1.47	0.186
2.0	0.63	1.04	3.31	1.51	0.198
2.5	0.73	1.14	3.35	1.56	0.212
3.0	0.83	1.25	3.40	1.68	0.228
3.5	0.94	1.36	3.45	1.73	0.244
4.0	1.06	1.49	3.51	1.83	0.261
4.5	1.19	1.62	3.57	1.97	0.280

Downloaded 16 Aug 2013 to 128.46.221.64. This article is copyrighted as indicated in the abstract. Reuse of AIP content is subject to the terms at: http://jap.aip.org/about/rights_and_permissions

TABLE III. Calculated direct and indirect band-gaps of YN using GW approximation calculation with different self consistency steps.

No. of self-consistent steps	$E_{\Gamma-X}$(eV)	E_X(eV)	E_Γ(eV)
1st	0.97	1.46	4.20
2_{nd}	1.14	1.66	4.50
3rd	1.20	1.72	4.58
4th	1.22	1.74	4.61

Freeman *et al.*,[8] however, gave an indirect bandgap of 0.85 eV. Using GGA coupled with a Hubbard U correction, we estimated both the direct and indirect bandgaps of YN as a function of U parameter. Estimates of bandgap presented (see Table II) show a monotonic increase in indirect and direct bandgaps as a function of U parameter. The indirect Γ-X bandgap of 0.83 eV and direct gap at the Γ and X point of 3.4 and 1.36 eV, respectively, estimated with $U = 3.0$ eV, are in good agreement with Freeman *et al.*'s[8] calculation. The values compare well with another theoretical calculation by Zerroug *et al.*,[9] who has reported an indirect gap of 0.80 eV using the EV-GGA technique.

Our calculations with the G_0W_0 approximation (see Table III) yield an indirect Γ-X bandgap of 0.97 eV and the direct gap at the Γ point of 4.2 eV and at the X point of 1.46 eV. As the number of self-consistent steps in the calculation is increased, these bandgaps increase (see Table III), and ultimately converge in the fourth cycle. We have already pointed out that self- consistent GW based estimations overestimate the band gaps, and hence we use only the results of the zeroth order in the self-energy (G_0W_0) corrections in the rest of the work.

Estimated electronic structure of YN along high symmetry directions of the Brillouin zone as a function of the Hubbard U parameter [see Fig. 1(a)] shows an increase in the indirect Γ-X bandgap. Direct gaps at the Γ and the X point of the dispersion spectrum also increase in the same manner. The dispersion resembles that of other transition nitride semiconductors like ScN[21] and LaN[8]. One obvious effect of the Hubbard U parameter is that the bandwidth of the 4-d Sc orbital becomes smaller with increasing U values. The dispersion along the Γ-X direction [see Fig. 1(b)] calculated using GGA, GGA + U with $U = 3.5$ eV, and G_0W_0 approaches compare well, apart from the fact that introduction of the Hubbard U parameter introduces a relatively larger gap along the Γ-X direction. The shapes of valence and conduction bands estimated using the G_0W_0 approach are similar to those obtained with GGA and GGA + U calculations.

The total densities of electronic states [see Fig. 2(a)] calculated using GGA + U (with $U = 3.5$ eV), and G_0W_0 are very similar, albeit a slight difference in the peak of the valence band N s-states. The valence bandwidth of N p-states is relatively larger for the G_0W_0 calculation compared to the results obtained from the GGA + U method. The partial density of states [see Fig. 2(b)] indicates a strong hybridization between the transition element d-states and nitrogen p-states with energy position and width of bands in the partial DOS for N and Y atoms appearing very similar.

To connect with the transport properties of YN relevant for thermoelectric applications, the longitudinal (m_l*) and transverse (m_t*) conduction band effective masses at the X point of the dispersion spectrum are calculated by fitting a quadratic function to the corresponding band energies along the (Γ-X) and the $Z(X$-$W)$ directions, respectively, and for different values of U parameters [see Table II]. Monotonic increase in effective masses with increasing U parameter is observed, consistent with the reduction in the d-bandwidth with increasing U parameter, (bands become more flat) resulting in the increase in effective mass found here. Our estimate of longitudinal conduction band effective mass (m_l*) at the X point of the dispersion spectrum using the G_0W_0 approximation is 1.19 m_0 (m_0 being the mass of free electron), slightly less than the one obtained with the GGA calculation without Hubbard corrections. To the best of our knowledge, the effective masses of YN have not been measured experimentally yet, neither is there any report of theoretical estimates of m_l* and m_t*. However, the calculated values are slightly lower than the theoretical estimates reported for ScN.[21]

As YN is being considered for forming alloys with other nitrides of different lattice constants, we have estimated the indirect and direct bandgaps as a function of its lattice constant using all three approaches, namely the G_0W_0 approximation and GGA and GGA + U with $U = 3.5$ eV. Results indicate an increase in indirect Γ-X bandgap, as well as direct gap at the X point, and a decrease in the direct gap at the Γ point, as we increase the lattice constant from − 2 to 2% with respect to the equilibrium values (see Fig. 3). The volume deformation potentials a_v^α for the band gaps

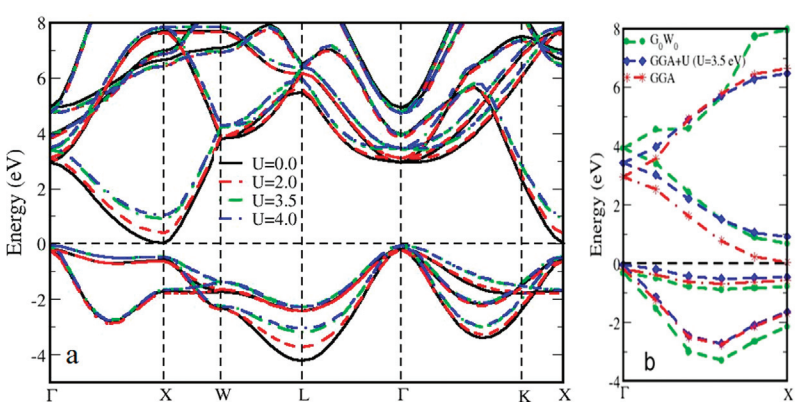

FIG. 1. (Color online) Electronic structure of YN calculated using GGA + U, and G_0W_0 approach. (a) The band diagram along the high symmetry directions of the Brillouin zone. (Hubbard U's are in units of eV.) (b) Comparison of the band diagram along Γ-X direction using GGA, GGA + U with $U = 3.5$ eV, and G_0W_0 approaches.

Downloaded 16 Aug 2013 to 128.46.221.64. This article is copyrighted as indicated in the abstract. Reuse of AIP content is subject to the terms at: http://jap.aip.org/about/rights_and_permissions

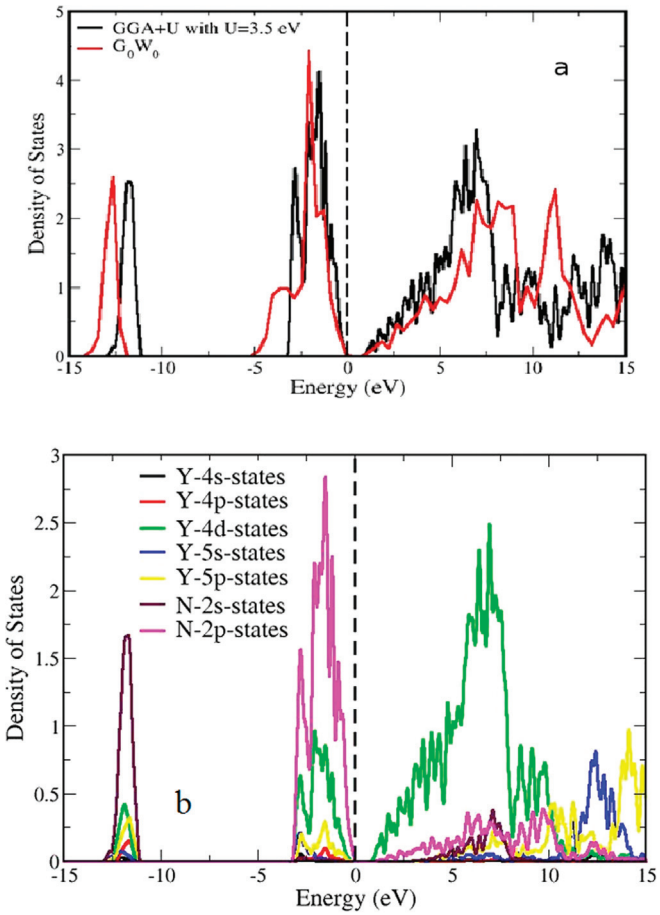

FIG. 2. (Color online) Electronic densities of states of YN. (a) The total densities of states calculated using the GGA + U method with $U = 3.5$ eV and the G_0W_0 approximation. (b) The partial densities of states, that is, the contribution of different atomic orbital's on DOS.

$E_E^{\Gamma-X}$, $E_g^{\Gamma-\Gamma}$, and E_g^{X-X} are calculated using the formula $dE_g^{\alpha}/dln(V/V_0)$, where V_0 denotes the volume of the unit cell at the equilibrium lattice constant and V is the volume of the strained lattice (see estimates in Table IV). We find that the volume deformation potentials do have dependence on the methodology employed. While no experimental estimates of

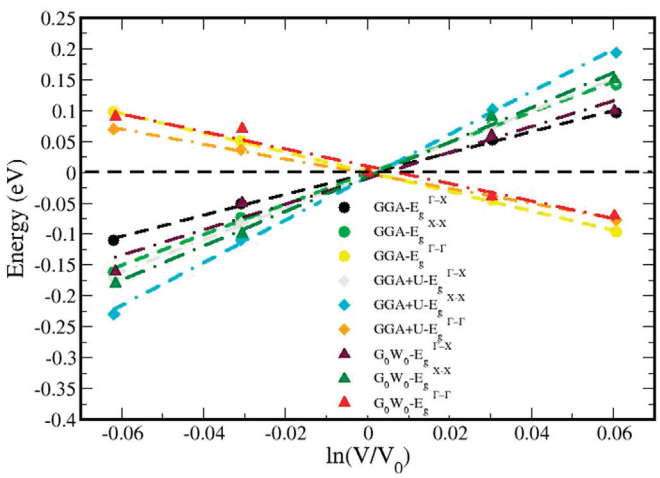

FIG. 3. (Color online) Changes in direct and indirect bandgaps as a function of change in the volume of the unit cell, calculated using GGA, GGA + U, and G_0W_0 approaches.

TABLE IV. Theoretical estimates of different band-gap volume deformation potential (a_v^{α}) (in eV) for YN using different methods.

Method used	$a_v^{\Gamma-X}$	$a_v^{\Gamma-\Gamma}$	$a_v^{X-X}a_v^{X-X}$
G_0W_0	2.07	1.41	2.79
GGA	1.68	1.57	2.47
GGA + U with $U = 3.5$ eV	2.60	1.20	3.45

the volume deformation potentials of YN are available, our results are comparable to those of ScN estimated by Qteish *et al.*[24] Their estimates of $E_g^{\Gamma-X}$, $E_g^{\Gamma-\Gamma}$, and E_g^{X-X} for ScN with OEPx(cLDA)-G_0W_0 are 2.02, 1.54, and 2.04 eV, respectively, whereas our estimates of the same with the G_0W_0 approach are 2.07, 1.41, and 2.79, respectively, for YN.

C. Vibrational spectrum

The vibrational spectrum of YN is essential to understand its potential for technological applications, particularly for developing thermoelectric and thermionic based solid state energy conversion devices. The phonon dispersion curve of YN (see Fig. 4) resembles that of ScN and is typical of those of rock salt structured materials with no anomaly. A long range dipole-dipole interaction is evident in the splitting of the longitudinal optical (LO) and transverse optical (TO) modes at the Γ point of the dispersion curve. Our estimates of the electronic dielectric constant ϵ^{∞} and Born effective charge of YN are 13.1 and 4.5, respectively, giving an LO-TO splitting of 335 cm^{-1}. Our result of $\omega^2_{LO}/\omega^2_{TO}$ at the Γ point is about 8.1, which is smaller than Isaev *et al.*'s[10] calculation of 10.1.

Although there is a large difference between the masses of Y and N, the acoustic and optical modes of dispersion spectrum are not separated by a gap, unlike the transition metal nitride of Zr, situated in the same row of the periodic table. This is similar to the presence of no gap in ScN,[21] however, there is a separation between acoustic and optical modes of YN, an interesting finding that can be utilized in modeling the thermal transport. The frequencies are however softer than those derived from the ScN dispersion spectrum, owing to the larger mass of Y compared Sc.

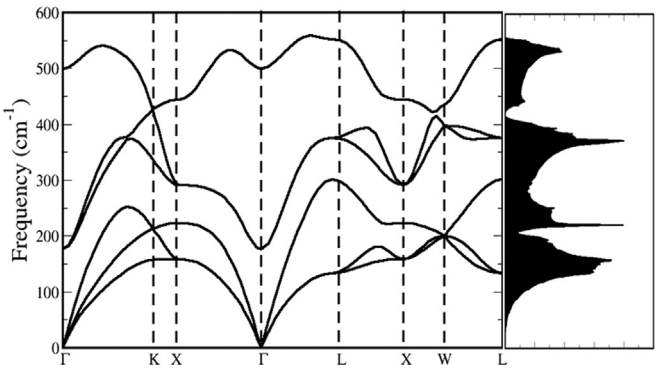

FIG. 4. Calculated phonon dispersion curve and density of states of YN in rock salt structure. First columns have the phonon dispersion curves, while the right column has phonon DOS with same frequency scale.

Downloaded 16 Aug 2013 to 128.46.221.64. This article is copyrighted as indicated in the abstract. Reuse of AIP content is subject to the terms at: http://jap.aip.org/about/rights_and_permissions

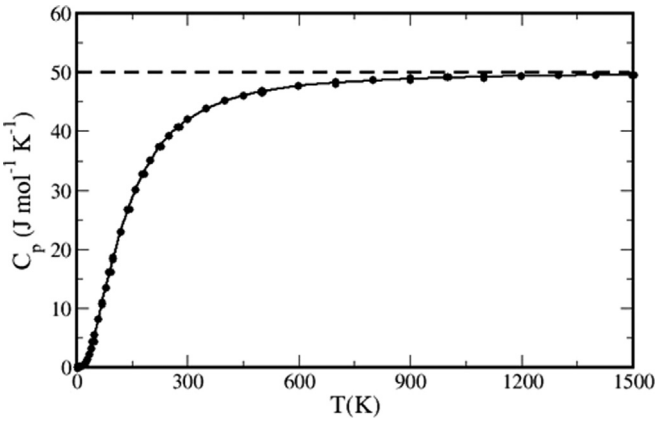

FIG. 5. Lattice specific heat as a function of temperature of YN. Horizontal line represents the classical Dulong-Petit limit of C_p.

D. Thermal properties

We now present theoretical estimates of lattice specific heat and lattice thermal conductivity, and we evaluate YN's potential for thermoelectric applications. Our estimate of the specific heat as a function of temperature for YN is shown in Fig. 5. The characteristic variation of C_p resembles that of other transition nitride materials like ScN, ZrN, HfN, and approaches the classical Dulong Petit value at higher temperatures. The Debye temperature (T_D) estimated using the acoustic branches of the dispersion curve is about 564 K for YN, a little lower than that of ScN, with T_D of 711 K.[21]

We now analyze the lattice thermal conductivity using Boltzmann transport theory. The scattering or the relaxation time, which derives from anharmonic interactions of phonons, is not readily estimated from first principles. We assume that the scattering time is constant for all phonons and analyze the thermal conductivity of YN, which includes only the effects of density of states and the group velocity of phonons. The estimated lattice thermal conductivity [see Fig. 6(a)] is slightly less than that of ScN,[21] but one order of magnitude higher than ZrN or HfN.[21] Because YN is semiconducting in nature, the estimated lattice C_p and κ should provide the primary contribution to their total values as the electronic contributions will be very small. The lattice thermal conductivity [see Fig. 6(a)] as a function of temperature does not change significantly at temperatures above 300 K. The frequency-dependent contribution of phonons to lattice thermal conductivity [see Fig. 6(b)] shows dominance of mid-frequency range (200–400 cm^{-1}) phonons in κ at high temperatures (above 100 K). At lower temperatures, long wavelength acoustic phonons dominate the lattice thermal conductivity.

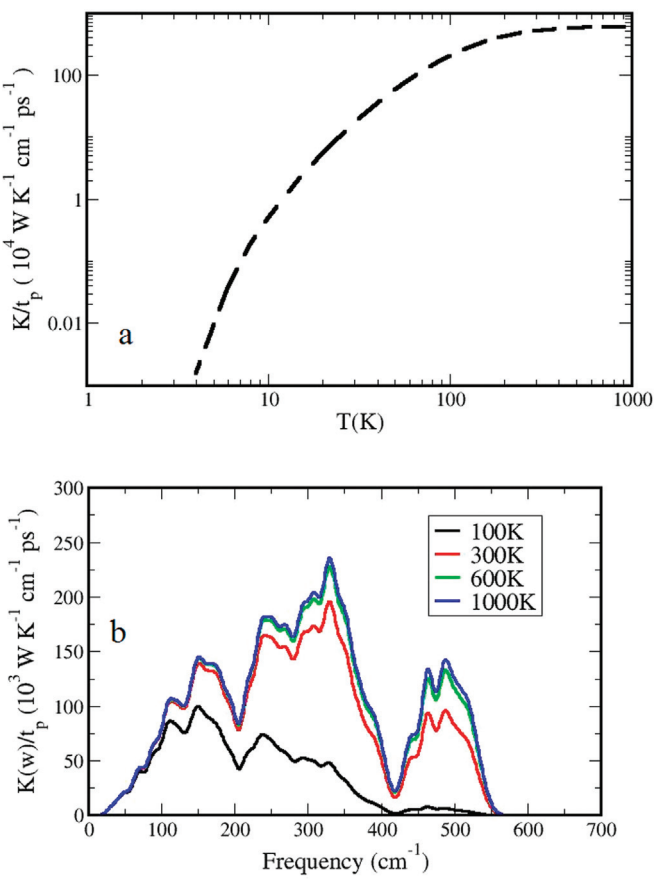

FIG. 6. (Color online) (a) Estimated lattice thermal conductivity as a function of temperature of YN. (b) Change in lattice thermal conductivity as a function of phonon frequencies.

IV. CONCLUSIONS

In conclusion, we have reported first-principles density functional theory based calculations of electronic structure, vibrational spectra, and thermal properties of YN with a motivation to understand its potential for thermoelectric applications. Our G_0W_0 results predict that YN is an indirect bandgap semiconductor with a Γ-X bandgap of 0.97 eV, suitable for applications in metal/semiconductor superlattices. To connect with transport properties, the longitudinal and transverse conduction band effective masses at the X point of the dispersion spectrum are determined as a function of Hubbard U parameter. Bandgap volume deformation potentials are calculated to determine YN's relevance for use in alloying in ScN based superlattices. Phonon dispersion, phonon density states, and thermal properties including lattice specific heat and lattice thermal conductivity (κ) and their dependence on temperatures are reported and discussed in comparison with properties of ScN.

ACKNOWLEDGMENTS

We thank IUS-STF for supporting collaborative interaction between JNCSAR and Purdue. Bivas Saha thanks JNCASR for a fellowship, and U.V.W. is thankful for funding from a DAE Outstanding Researcher Grant.

[1]H. F. George and H. K. John, Phys. Rev. **93**, 1004 (1954).
[2]A. Nigro, G. Nobile, V. Palmieri, G. Rubino, and R. Vaglio, Phys. Scr. **38**, 483 (1988).
[3]K. Kawaguchi and M. Sohma, Jpn. J. Appl. Phys., Part 2 **30**, 2088 (1991).
[4]K. Wakasugi, M. Tokunaga, T. Sumita, H. Kubota, M. Nagata, and Y. Honda, Physica B **239**, 29 (1997).
[5]V. Rawat, Y. Koh, D. Cahill, and T. Sands, J. Appl. Phys. **105**, 024909 (2009).
[6]M. Zebarjadi, Z. Bian, R. Singh, A. Shakourie, R. Wortman, V. Rawat, and T. Sands, J. Electron. Mater. **38**, 960 (2009).

Downloaded 16 Aug 2013 to 128.46.221.64. This article is copyrighted as indicated in the abstract. Reuse of AIP content is subject to the terms at: http://jap.aip.org/about/rights_and_permissions

[7]L. Mancera, J. A. Rodriguez, and N. Takeuchi, J. Phys. Condens. Matter **15**, 2625 (2003).
[8]C. Stampfl, W. Mannstadt, R. Asahi, and A. J. Freeman, Phys. Rev. B **63**, 155106 (2001).
[9]S. Zerroug, F. Ali Sahraoui, and N. Bouarissa, Appl. Phys. A **97**, 345 (2009).
[10]E. I. Isaev, S. I. Simak, I. A. Abrikosov, R. Ahuja, Yu. Kh. Vekilov, M. I. Katsnelson, A. I. Lichtenstein, and B. Johansson, J. Appl. Phys. **101**, 123519 (2007).
[11]S. Duman, S. Bagci, H. M. Tutuncu, G. Ugur, and G. P. Srivastava, Diamond Relat. Mater. **15**, 1175 (2006).
[12]V. I. Anisimov and O. Gunnarson, Phys. Rev. B **43**, 7570 (1991).
[13]M. Shishkin and G. Kresse, Phys. Rev. B **75**, 235102 (2007).
[14]M. Shishkin and G. Kresse, Phys. Rev. B **74**, 035101 (2006).
[15]J. P. Perdew, K. Burke, and M. Ernzerhof, Phys. Rev. Lett. **77**, 3865 (1996).
[16]X. Hua, X. Chen, and W. A. Goddard III, Phys. Rev. B **55**, 16 (1997).
[17]D. Vanderbilt, Phys. Rev. B **41**, 7892 (1990).
[18]H. J. Monkhorst and J. D. Pack, Phys. Rev. B **13**, 5188 (1976).
[19]M. Methfessel and A. Paxton, Phys. Rev. B **40**, 3616 (1989).
[20]S. Baroni, S. de Gironcoli, A. Dal. Corso, and P. Giannozzi, Rev. Mod. Phys. **73**, 515 (2000).
[21]B. Saha, J. Acharya, T. Sands, and U. V. Waghmare, J. Appl. Phys. **107**, 033715 (2010).
[22]G. Kresse and J. Furthmüller, Phys. Rev. B **54**, 11169 (1996).
[23]P. Villars and L. D. Calvert, *Pearsons Handbook of Crystallographic Data for Intermetallic Phases* (American Society for Metals, Metals Park, Ohio, 1985).
[24]A. Qteish, P. Rinke, M. Scheffler, and J. Neugebauer, Phys. Rev. B **74**, 245208 (2006).

Downloaded 16 Aug 2013 to 128.46.221.64. This article is copyrighted as indicated in the abstract. Reuse of AIP content is subject to the terms at: http://jap.aip.org/about/rights_and_permissions